

Time-resolved, light scattering measurements of cartilage and cornea denaturation due to free electron laser radiation

Emil Sobol

Alexander Sviridov

Moishe Kitai

Research Center for Technological Lasers
Russian Academy of Sciences
Pionerskaya 2
Troitsk, Moscow Region, 142092
Russian Federation
E-mail: sobol@laser.ru

Jonathan M. Gilligan

Norman H. Tolk

Glenn S. Edwards

Vanderbilt University
P.O. Box 1816 Station B
Nashville, Tennessee 37235

Abstract. Light scattering is used to monitor the dynamics and energy thresholds of laser-induced structural alterations in biopolymers due to irradiation by a free electron laser (FEL) in the infrared (IR) wavelength range 2.2 to 8.5 μm . Attenuated total reflectance (ATR) Fourier-transform IR (FTIR) spectroscopy is used to examine infrared tissue absorption spectra before and after irradiation. Light scattering by bovine and porcine cartilage and cornea samples is measured in real time during FEL irradiation using a 650-nm diode laser and a diode photoarray with time resolution of 10 ms. The data on the time dependence of light scattering in the tissue are modeled to estimate the approximate values of kinetic parameters for denaturation as functions of laser wavelength and radiant exposure. We found that the denaturation threshold is slightly lower for cornea than for cartilage, and both depend on laser wavelength. An inverse correlation between denaturation thresholds and the absorption spectrum of the tissue is observed for many wavelengths; however, for wavelengths near 3 and 6 μm , the denaturation threshold does not exhibit the inverse correlation, instead being governed by heating kinetics of tissue. It is shown that light scattering is useful for measuring the denaturation thresholds and dynamics for different biotissues, except where the initial absorptivity is very high. © 2003 Society of Photo-Optical Instrumentation Engineers.

[DOI: 10.1117/1.1559996]

Keywords: cartilage; cornea; laser-tissue interaction; denaturation; light scattering; absorption spectra.

Paper JBO 01083 received Dec. 12, 2001; revised manuscript received Jun. 24, 2002; accepted for publication Sep. 20, 2002

1 Introduction

Cartilage and cornea are glycopolymer and protein-based systems with native macromolecular structures that are of great importance for their functional properties. Localized laser ablation and modification of biological tissues are being widely used in surgery and medicine. It is well known that laser heating may result in thermal decomposition of biopolymers, where the rate of interatomic bond breakage rises rapidly with temperature. The broken bonds recover in part, but diffusive atomic motions and macromolecular displacements hamper the recovery of the broken bonds and make the denaturation process irreversible. Various lasers are being used for the treatment of different biological tissues, but the optimal wavelength to selectively modify tissue structure is often unknown.

The threshold and dynamics of laser-induced denaturation of biopolymers are extremely important characteristics for determining optimal laser wavelengths for various applications of lasers in medicine. Tissue denaturation by IR lasers is a thermally and mechanically mediated process that sets an upper bound for low-energy procedures, such as reshaping of cartilage, and determines the thermal damage for high-energy laser processes, such as tissue ablation and welding.^{1–3} Laser-induced alteration of tissue structure changes the number and size of light-scattering centers in the tissue. It allows us to consider denaturation as an alteration in organization of tissue

native structure and to study the process by means of optical techniques. The characteristic size of proteoglycan units (hundreds of nanometers) and aggregates ($\sim 1 \mu\text{m}$)⁴ are near the wavelength of visible light, making cartilage and cornea well suited biopolymers for light scattering.

The laser light-scattering technique has been widely used for structural characterization of proteoglycans in solutions^{5–7} and for investigations of laser-induced stress relaxation in cartilage.^{8,9} A strong correlation between light scattering and mechanical properties of cartilage was documented.¹⁰ At present, the data on the correlation between light scattering and rapid structure alteration in biotissues under pulse laser radiation are very limited. The current work is focused on denaturation of cartilage and corneal tissue with a free electron laser (FEL) in the wavelength region 2.2 to 8.5 μm . The aim is to determine the wavelength dependence of threshold irradiance for inducing denaturation and of kinetics of denaturation.

2 Materials and Methods

Fresh bovine and porcine nasal septums and eyes were used to prepare samples of hyaline cartilage and cornea. Separated nasal septums and eyes were placed between gauze sponges

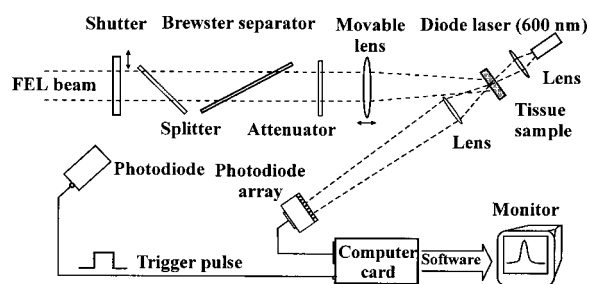


Fig. 1 Experimental setup for real-time light scattering monitoring of tissue denaturation under laser radiation.

soaked in 0.9% saline and stored at 2 to 4 °C in a closed box. All tissues were within 24 hours after the animal was sacrificed. The samples for investigation were prepared immediately before experiment by cutting out disks of 9.8 mm in diameter with a thickness of 1.3 mm for cartilage, of 0.9 mm for porcine cornea, and of 1.2 mm for bovine cornea. The samples were mounted to irradiate an area 6 mm in diameter. A total of 160 samples, including 100 bovine nasal cartilages, 20 porcine nasal cartilages, 32 bovine cornea, and 8 porcine cornea, were harvested from two pigs and five bovines for the experiment.

Every sample was used only for one irradiation procedure. Eight cartilage samples ($2.4 \times 5 \times 25 \text{ mm}^3$) from a bovine nasal septum were prepared for FTIR measurements.

The experimental setup is presented in Fig. 1. The Vanderbilt Mark-III FEL¹¹ is tunable from 2 to 10 μm . The Mark-III FEL produces a superpulse (macropulse), comprised of a train of micropulses, each approximately 1 ps long and separated by 350 ps. The macropulse lasts 3 to 6 μs and is characterized by both high-average and high-peak power. The maximum macropulse energy ranges from 10 to 100 mJ, depending on wavelength. The macropulse can be repeated at up to 30 Hz. The typical energy of the superpulse used in our experiments was 20 to 30 mJ and the pulse repetition rate was 20 Hz. The mode structure of the emitted IR beam is TEM_{00} . The FEL was used for sample irradiation in the wavelength range from 2.2 to 8.5 μm . The following wavelengths were used for tissue irradiation: 2.2, 2.5, 2.81, 3.0, 3.22, 3.5, 3.9, 4.68, 5.3, 6.0, 6.1, 6.45, 6.7, 6.85, 7.2, 7.4, 7.8, 8.05, and 8.5 μm . The FEL beam passed through a germanium Brewster separator that reflects $1/n$ harmonics and transmits FEL radiation.

The FEL beam was focused using a BaF_2 lens of 272-mm focal length in the visible region. In the wavelength region of FEL radiation it varied about 30 mm due to the wavelength dependence of the BaF_2 refractive index. Therefore the sample was located at an appropriate distance ahead of the lens focus to provide 2.5 mm of the effective diameter of the FEL beam at the $1/2$ level for every particular wavelength used. This distance was estimated using a geometrical consideration of triangles similarity using an initial FEL beam diameter and appropriate focal length of focusing lens. An FEL pulse has approximately trapezium-like spatial distribution in the far field, and the averaged laser irradiance was estimated as the full energy of the laser pulse divided to the square of the circle of 2.5 mm diameter.

The Fresnel attenuator, consisting of a number of CaF_2 plates, was used to control the FEL power. All samples irra-

diated were examined with a Zeiss surgical microscope, Universal S3 (Germany), with magnification of $60\times$ to investigate any visible alterations of the surface.

The essential measurement is the time evolution of the intensity distribution of visible light passing through a sample during irradiation with the infrared FEL. The 650-nm light of the laser pointer was focused on the backside of a sample by a lens of 190-mm focal length to a spot of 1 mm in diameter. Another lens of 80-mm focal length and 50 mm diameter was used to image the front surface of the sample on the plane of a photodiode array with magnification of 2.8. Thus the fraction of the probe beam that direct scattered in the aperture angle of this lens (~ 0.46), together with nonscattered fraction, contribute to the image on the array plane, giving the proportional value of actual intensity distribution on the sample surface. Such an approach suggests that angular distribution of scattered fraction is not changed strongly with the distance from the beam axis.

The photodiode array included 3700 elements located along a line with 8- μm distance between neighboring elements, which is much more sensitive to small changes in scattered light distribution than a simple photodiode with a large measurement area. The light intensity distribution was registered using a "Multichannel Optical Registration System" and the software produced by MORS Limited, Russia. The computer card was operated in the regime of external triggering. The triggering pulse was generated simultaneously with the opening of a shutter, recording a series of images of light intensity distribution on the plane of the photodiode array in the frame series mode. Every frame was exposed from 50 to 250 ms. The repetition rate of frame recording was 4 Hz for most of the experiments: 1-Hz repetition rate of frame recording was used when required. The recording time was 20 s. Typically 80 images for each sample irradiation were captured and analyzed. To decrease the effect of individual variability of tissue samples derived from different animals, we studied the dynamics of the relative alterations of the light scattering in the tissue samples during irradiation.

Attenuated total reflectance (ATR) FTIR spectra of 2.4-mm-thick cartilage samples were measured before and after irradiation at 6.0 and 2.2 μm . Several samples irradiated with the FEL at 6.0 μm (when the absorption coefficient is high) and at 2.2 μm (with small absorption) were examined with a Bruker IFS 66 V. Tissue was irradiated with a 2.5-mm-diam FEL spot at the laser radiant exposure F of about 0.6 J/cm^2 per pulse for 15 s. Then the FEL beam was moved 2.5 mm along the central line of the $5 \times 25 \text{ mm}^2$ sample surface, the next spot was irradiated, and the process was repeated.

3 Results and Discussion

3.1 Evolution of Light Scattering

Cartilage and cornea have very similar absorption spectra. Both of these tissues are comprised of water, collagen, and proteoglycans, but have different secondary and tertiary (organizational) structures. This makes these tissues interesting for comparative examination of laser-induced structural alterations using the light scattering technique. Figure 2 is an example of the time course of the intensity distribution of light passing through a sample during FEL irradiation. Figure 2 shows the intensity of light transmitted, and the loss of light

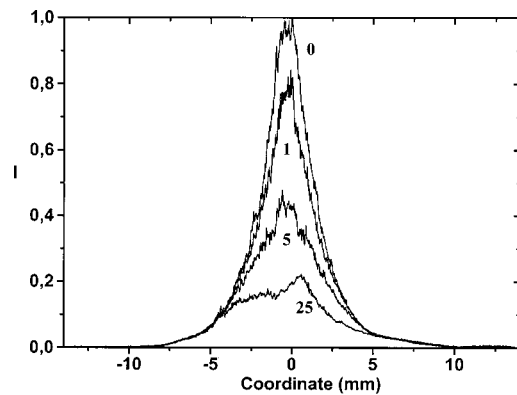


Fig. 2 The spatial distribution of a probe beam at the plane of a photodiode array (magnification $\times 2.8$) and its alternations by cartilage irradiated by FEL. The numbers refer to the duration of the irradiation (in seconds); FEL wavelength $\lambda = 8.5 \mu\text{m}$, pulse radiant exposure $F = 0.23 \text{ J/cm}^2$, $f = 20 \text{ Hz}$. I is the intensity of the visible scattered light in arbitrary units, and Coordinate is the position on the photodiode array in millimeters.

transmitted is due to an increase of light scattering in the tissue sample. From these (and other data of a similar nature), we have analyzed the dynamics of light scattering, in particular the maximal light intensity (I_m), the half width (w), and the 2-D integral on the intensity distribution of the scattered light (A). The 2-D integral was defined on the assumption that there exists a cylindrical symmetry of the intensity distribution of the scattered probe beam, and the photodiode array records the 1-D cross section of this distribution. The results show that the 2-D integral is a more reliable parameter to characterize the tissue denaturation. Some of the time dependencies of A are plotted in Figs. 3 and 4 for different laser wavelengths and radiant exposures. All experiments have been repeated two to three times. The procedure of averaging has been carried out not at the stage of initial processing of the experimental data, but at the stage of determining essential kinetic parameters.

Figures 2–4 indicate that the light distribution becomes broader and the intensity of light passing through a sample decreases with time and increasing FEL radiant exposure. It represents an increase in the light scattering due to structural alterations in tissue being irradiated. For small F , neither were alterations in light distribution seen during the period of observation, nor were visible changes on the irradiated surface observed using a light microscope. For higher F values, we have observed partial whitening of the irradiated spot and visible alterations in I_m , and A commence with a delay depending on laser radiant exposure and wavelength λ (Figs. 3 and 4). However, we did observe this trend to reverse (at $t > t_a$). Results of experiments for $F = 0.29 \text{ J/cm}^2$, and for $\lambda = 5.30 \mu\text{m}$, and also for $F = 0.38 \text{ J/cm}^2$, $\lambda = 8.05 \mu\text{m}$ are found more specifically. Under these conditions, we observed a hollow and darkening on the tissue surface irradiated. Plausible explanations for the observed reversal include tissue dehydration preceding the onset of carbonization, the onset of ablation resulting in decrease of optical density of the sample, or a change in the length distribution of scattering centers. Since tissue carbonization itself cannot be responsible for decrease in optical density, the carbonization is accompanied by

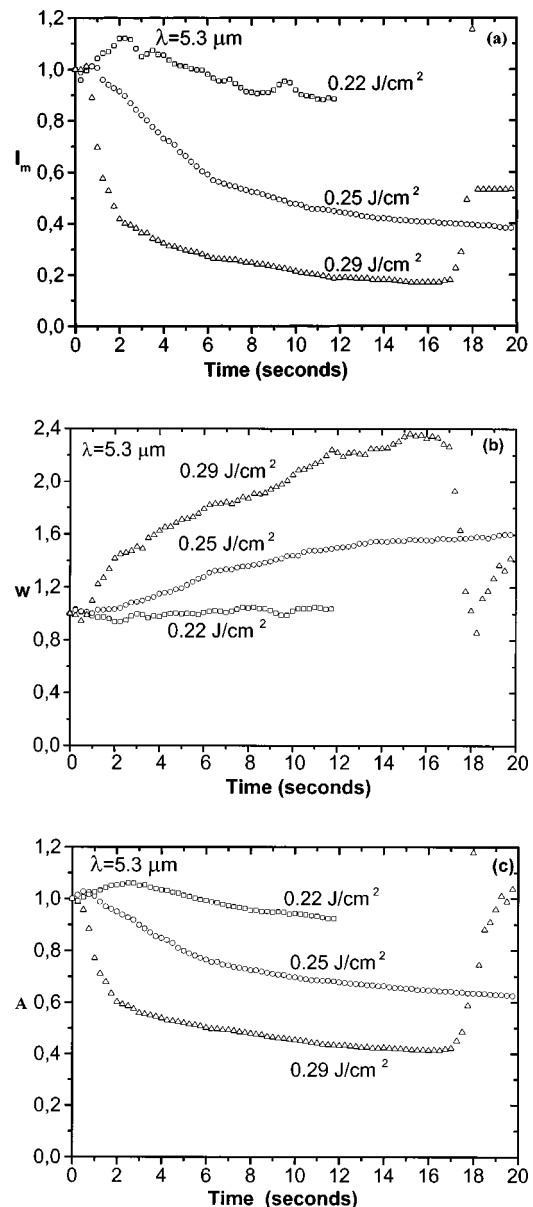


Fig. 3 Kinetics of relative intensity of the light scattering in cartilage as a function of FEL pulse radiant exposure (noted at the curves) for $\lambda = 5.30 \mu\text{m}$: (a) maximal value of scattered light intensity I_m versus the time of irradiation (in seconds); (b) half-width w of the scattered light distribution versus the time of irradiation (in seconds); and (c) 2-D integral of the intensity distribution of scattered light A versus the time of irradiation (in seconds).

a sharp increase in the absorption coefficient. This accelerates the heating of tissue a number of times and may result in tissue ablation.¹

3.2 Time Delay of Tissue Denaturation

We defined the denaturation delay time t^* in the first instance as the value when A drops up to 10% of its initial value. Plotting t^* as a function of F (Fig. 5), we have found the value of the denaturation threshold F_{th} , which is determined

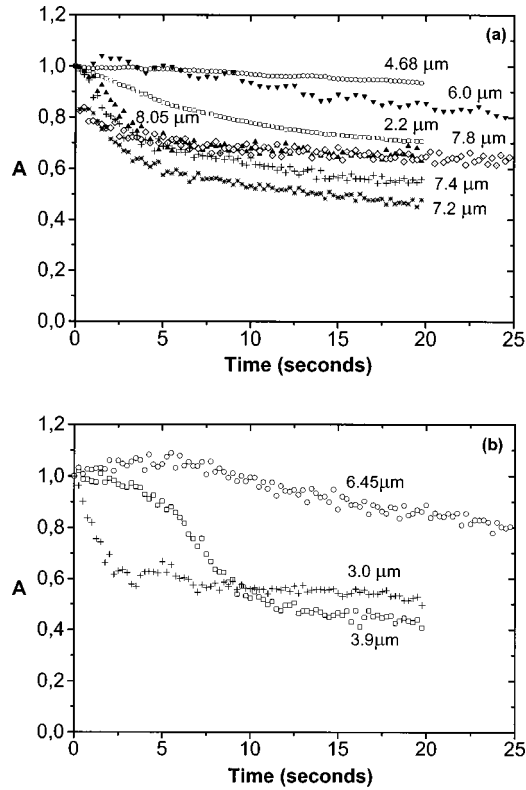


Fig. 4 Kinetics of the 2-D integral A (normalized to the initial value) versus time of irradiation (in seconds) as a function of wavelengths (noted at the Figure) at $F \approx 0.1 \text{ J/cm}^2$, for (a) cartilage at (b) cornea.

as an asymptotic laser radiant exposure when t^* tends to infinity. The curves on Fig. 5 fit to the experimental data with the function

$$t^* = t_0 + B/(F - F_{th})^2, \quad (1)$$

where t_0 , B , and F_{th} are constants. The relation is deduced in what follows.

Assume that t^* is the sum of two values: t_h is the time necessary to heat a tissue surface up to a certain temperature T_d for which the denaturation starts, and t_0 is the minimal time necessary for redistribution of tissue structural elements. According to the model of the diffusion-limited denaturation of biopolymers under laser radiation,¹² $t_0 \approx L^2/D$, where L is a characteristic size of the structural alterations in a tissue, and D is an effective diffusion coefficient of moving structural elements. Following Ref. 12 and using, for the estimation of denaturation of the cartilage, $L \approx 5 \mu\text{m}$, $D \approx 10^{-6} \text{ cm}^2/\text{s}$, we get $t_0 \approx 0.25 \text{ s}$, which is much smaller than a characteristic time of our experiments.

The calculation of t_h has been described in detail elsewhere (Ref. 1, Sec. 1.2). When the inequality $\alpha(at_h)^{1/2} \gg 1$ is true and we are ignoring the thermal effect of water evaporation (see Ref. 12), the simple expression for the superficial temperature can be used¹

$$T_d = T_0 + (2Ff/\chi)(at_h/\pi)^{1/2}, \quad (2)$$

where $T_0 = 25^\circ\text{C}$ is the initial “room” temperature, χ and a are tissue thermoconductivity and thermodiffusivity coeffi-

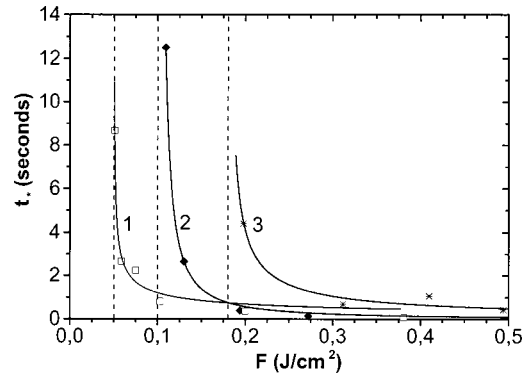


Fig. 5 Denaturation delay time t^* (in seconds) versus the pulse radiant exposure F (in J/cm^2) for cartilage: (1) $\lambda = 8.05 \mu\text{m}$, (2) $\lambda = 6.00 \mu\text{m}$, and (3) $\lambda = 2.50 \mu\text{m}$. The solid curves are calculated in accordance with the function $t^* = t_0 + B/(F - F_{th})^2$. The denaturation threshold F_{th} is determined as an asymptotic pulse radiant exposure when denaturation delay tends to infinity.

icients, α is the tissue coefficient of absorption, and f is the pulse repetition rate. From Eq. (2), it follows: $t_h = B/F^2$, where $B = \pi[(T_d - T_0)\chi]^2/4af$. At $t_h \gg t_0$ and $F \gg F_{th}$, the last formulas coincide with Eq. (1).

Setting the measurement time t_m to t_h , we obtain an expression for F_{th} :

$$F_{th} = (B/t_m)^{1/2}. \quad (3)$$

3.3 Wavelength Dependencies

For $\chi = 5 \times 10^{-3} \text{ W/K} \cdot \text{cm}$, $a = 1.4 \times 10^{-3} \text{ cm}^2/\text{s}$, $T_d = 70^\circ\text{C}$ ¹² and for experimental conditions used $f = 20 \text{ Hz}$, $t_m = 20 \text{ s}$, formula (3) gives $F_{th} \approx 0.1 \text{ J/cm}^2$, which is quite close to the experimental values of the denaturation threshold for FEL wavelengths near the 2.9- and 6.1- μm water absorption bands, where the absorption α is relatively high and the inequality $\alpha(at_h)^{1/2} \gg 1$ is true. For other IR wavelengths, this inequality is not obeyed. The wavelength dependence of F_{th} and the absorption spectrum of cartilage are shown in Fig. 6(a).

It should be noted that the minimal experimental value of $F_{th} = 0.03 \text{ J/cm}^2$ has been observed at $\lambda = 6.45 \mu\text{m}$. It could be due to the heterogeneous absorption of light by different components of cartilage. The specific absorption of collagen for $\lambda = 6.45 \mu\text{m}$ and its effect on laser-tissue interaction was previously established and discussed in Ref. 13.

When the IR light absorption depth is not very small compared to the thickness of a sample, denaturation starts in a layer of $1/\alpha$ in thickness, and the minimal time for denaturation is t_0 . For the onset of the denaturation process and when the relation $\alpha(at)^{1/2} \ll 1$ is true, the depth heated under laser radiation is governed mainly by the absorption depth $1/\alpha$, and instead of Eqs. (2) and (3) we should write¹

$$T_d = T_0 + F_{th}\alpha ft_0/C, \quad (4)$$

$$F_{th} = C(T_d - T_0)/\alpha ft_0.$$

Formula (4) predicts: $\alpha F_{th} = B_1$, where $B_1 = C(T_d - T_0)/ft_0$ must be constant. For $f = 20 \text{ Hz}$, $t_0 = 0.25 \text{ s}$, C

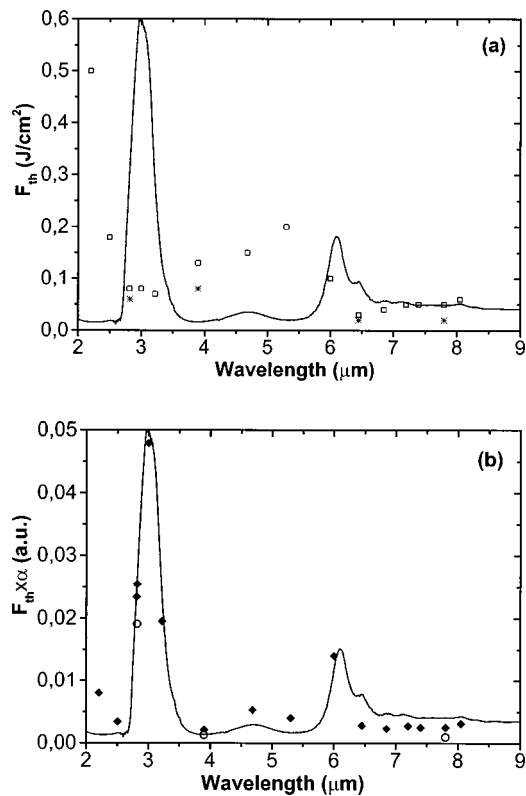


Fig. 6 Dependency of denaturation threshold F_{th} (in J/cm^2) as a function of wavelength λ (in μm); the plotted solid curve is the absorption spectrum for cartilage in arbitrary units: (a) F_{th} versus λ ; (\square) cartilage, ($*$) cornea; and (b) composition αF_{th} versus λ ; (\bullet) cartilage and (\circ) cornea.

$=4.2 \text{ J}/\text{cm}^3 \text{ K}$, $T_d - T_0 = 45^\circ \text{C}$ (see previous), we get $B_1 = 38 \text{ J}/\text{cm}^3$, which agrees with the experimental values of αF_{th} versus λ plotted in Fig. 6(b). An inverse correlation between denaturation thresholds and the absorption spectrum of the tissue is observed for many wavelengths examined, with the exception of the wavelength regions near the 2.9- and 6- μm water absorption bands, where the absorption coefficient was relatively high. The experimental values of $B_1 = 36 \pm 12 \text{ J}/\text{cm}^3$ are in good agreement with the calculated value. Here the α values have been calculated from the absorption spectrum shown in Fig. 6, assuming that 3- μm laser radiation has been absorbed mainly by water. It is not surprising that, for relatively high α , the denaturation threshold is not inversely proportional to the absorption coefficient.

3.4 Approximate Description of the Denaturation Dynamics

The Arrhenius formalism is often used for the description of the kinetics of various chemical reactions, including the reaction of denaturation.^{14–16} The rough approximation of the activation energy of cartilage denaturation using the data presented in Fig. 7 gives $E_a \approx 180 \text{ kJ}/\text{mol}$. This value correlates with the values determined for the denaturation of cornea^{14,15} $E_a \approx 106 \text{ kJ}/\text{mol}$, and liver $E_a \approx 260 \text{ kJ}/\text{mol}$.¹⁶ The typical values of activation energy of denaturation lie between 100 and 400 kJ/mol .¹⁶ Generally, tissue denaturation is a multi-stage, diffusion-limited reaction accompanied by the complex

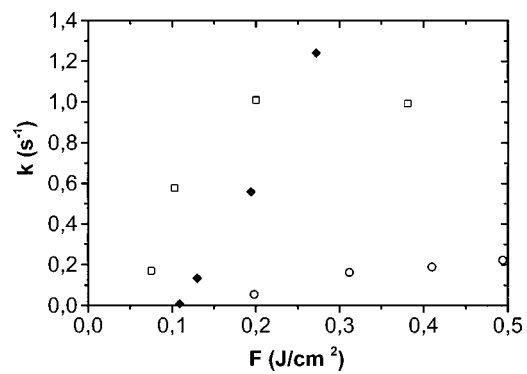


Fig. 7 Dependency of kinetic coefficient k (in inverse seconds) on pulse radiant exposure F (in J/cm^2) for cartilage: (\square) $\lambda = 8.05 \mu\text{m}$; (\bullet) $\lambda = 6.00 \mu\text{m}$; and (\circ) $\lambda = 2.5 \mu\text{m}$.

motion of macromolecules and their segments.^{1,12} This reaction cannot be described adequately with the Arrhenius formalism. In particular, the Arrhenius formalism does not allow describing the existence of the threshold of denaturation. It has been noted elsewhere¹⁷ that a single kinetic rate process may not be indicative in the description of the coagulation process. Actually, the Arrhenius formulas, taking into consideration only the single-stage unidirectional reaction, can be used only as a first approximation of the complex, multistage process. We limit ourselves with a simple consideration based on the phenomenological equations of thermoconductivity and phase transformations.¹ A dynamic approach should consider nucleation and growth of the light scattering centers and take into account that denaturation occurs in the heated layer, where the thickness depends both on light absorption depth and on heating kinetics in the tissue, and also that dynamics of denaturation is diffusion dependent.¹ Nonetheless, Eqs. (3) and (4) account for several features of the experimental results, in particular the denaturation threshold.

The rate constant or kinetic coefficient k can be found from a standard, approximate model for kinetics:

$$A = A_u + (1 - A_u) \exp(-kt). \quad (5)$$

Here A_u is the minimal value of the $A(t)$ function, k is a function of laser wavelength (Fig. 8) and radiant exposure (Fig. 7), and t is the variable time counted from the moment, when it has completed the time necessary to heat the tissue surface up to a certain temperature $T_d \approx 70^\circ \text{C}$ for which the denaturation starts (before this value has been noted as t_h). To exclude the nonsteady-state effects, all calculations of the k values were carried out using the time dependencies of A during the time interval: $t^* < t < t_a$, where once again t^* is the denaturation delay and t_a is the instance when the process of ablation starts.

Equation (5) can be derived from the first order phase transformation kinetics¹

$$d\eta/dt = -k(1 - \eta), \quad (6)$$

under an assumption that the integral of light intensity going through a sample obeys the following relation with the denaturation kinetics: $A(t) = 1 - (1 - A_u)\eta$, or, in other words, the differential of A is proportional to the amount of nondenatured

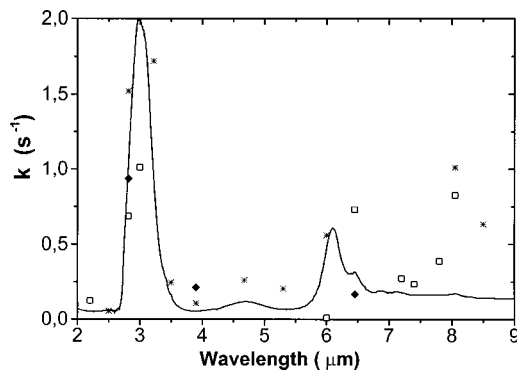


Fig. 8 Kinetic coefficient k (in seconds) as a function of FEL wavelength λ (in μm): (\square) cartilage, $F \approx 0.1 \text{ J/cm}^2$; (\bullet) cornea, $F \approx 0.1 \text{ J/cm}^2$; and ($*$) cartilage, $F \approx 0.2 \text{ J/cm}^2$.

tissue: $(A - A_u)/(1 - A_u) = 1 - \eta$. Here η is the fraction of the bulk of tissue that undergoes denaturation, and k is the rate constant. $A = 1$ at $\eta = 0$, and $A = A_u$ at $\eta = 1$.

This rough description allows us to characterize the denaturation kinetics with only one coefficient k and to investigate the effect of laser fluence and wavelength on k (Figs. 7 and 8). From Eq. (6) we have $k = d\eta/dt$ at $\eta = 0$.

Typically, k is a temperature-dependent value interpreted in terms of a molecular mechanism. We do not consider different models for rate constant, but present simple formulas that allow us to understand the wavelength dependence of the denaturation rate. In our experiments the exposure time is much longer than the characteristic diffusion time t_0 . As a first approximation, let $\eta = H/H_0$, where H_0 is the tissue sample thickness, and H is the thickness of a layer denatured under laser radiation. The exact (but quite complicated) formulas to calculate H are presented elsewhere.^{1,13}

For a high absorption coefficient, the absorption depth is very small, and we can write for the first approximation:¹ $H \approx vt$, where $v \approx Ff/Q_d$ is the moving velocity of the denaturation front, and Q_d is the denaturation heat per tissue volume. For high α , it follows that $k = d\eta/dt \approx v$ is proportional to F , which is in agreement with the data shown in Fig. 7 (for $\lambda = 6 \mu\text{m}$). When the absorption coefficient is not very high, the denaturation cannot be described with such a simple formula, since the kinetics of the process depend both on the initial absorption depth and on laser fluence. This suggests an explanation for the observation that when α is small, k does not depend strongly on the radiant exposure, as is the case for high α (Fig. 7).

It is also seen in Fig. 7 that k goes to zero with decreasing F . This could be another way to determine denaturation thresholds. The values of F_{th} obtained from the fluence dependencies of k are similar to the values F_{th} found from the dependencies of t^* on F . [They differ by no more than 30% from those shown in Fig. 6(a).]

The results presented in Fig. 8 indicate that there is a tendency for k to increase with the absorption coefficient, and that the rate of denaturation can be tuned by wavelength. For example, k is higher for $6.45 \mu\text{m}$ than for $6.0 \mu\text{m}$, inversely correlating with the wavelength dependence of the absorption coefficients. As we mentioned before, this may be due to the specific absorption of collagen for $6.45 \mu\text{m}$ established and

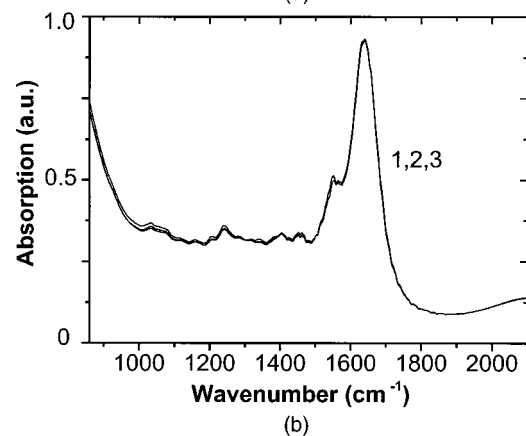
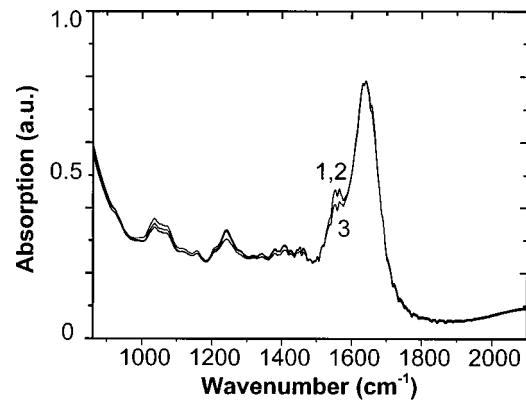


Fig. 9 ATR FTIR spectra of cartilage: (1) nonradiated sample, (2) back surface of the irradiated sample, and (3) front surface of the irradiated sample for the FEL wavelengths of (a) $6.00 \mu\text{m}$ and (b) $2.2 \mu\text{m}$. The ATR spectra are scaled for a coincidence of the top of water peak at 1640 cm^{-1} and of the base from the right hand of this peak.

discussed elsewhere.¹³ It is interesting to note the relatively high values of k were found for wavelengths near $8 \mu\text{m}$, where 7.5 to $8.2 \mu\text{m}$ is the wavelength range for the amide III band.¹³

3.5 IR Absorption Spectra

Figure 9 presents the ATR spectra of 2.4-mm-thick cartilage samples measured before and after irradiation at 6.0 and $2.2 \mu\text{m}$. At $6.0 \mu\text{m}$, where the absorption is relatively high, the spectrum of the irradiated (front) surface shows changes. In comparison, the spectrum of the back surface was identical to that before irradiation. We attribute this difference to pyrolytic denaturation at the front surface due to laser heating in a small absorption depth. At $6.0 \mu\text{m}$, we overheated the irradiated surface to produce significant light scattering. As the sample was thick enough to heat the back surface, the spectrum of the back surface was identical to that before irradiation. For $2.2\text{-}\mu\text{m}$ irradiation, where the absorption is relatively small, the spectrum of the front and back surfaces of the irradiated sample were unchanged from before irradiation, although light scattering indicates the onset of denaturation. These observations suggest that the absorption is too small to produce measurable alteration of structure. Furthermore, we conclude that the light scattering technique is more sensitive than the

spectroscopic FTIR technique for studying the onset of denaturation, when laser energy is much higher than the threshold of denaturation.

4 Summary

The effect of laser wavelength on energy threshold and kinetic coefficients for cartilage and cornea denaturation is studied for the first time. We found that while cartilage and cornea have similar absorption spectra, the denaturation threshold for cornea is slightly lower than that for cartilage. An inverse correlation between denaturation thresholds and the absorption spectrum of the tissue is observed for much of the spectrum; however, near the 2.9- and 6- μm bands, the denaturation threshold is not inversely proportional to the absorption coefficient. The largest rate constants for denaturation are observed for wavelengths corresponding to water absorption bands, to the amide III band, and, to a lesser extent, the amide II band. Light scattering is a more sensitive technique than ATR FTIR for measuring denaturation thresholds and kinetics for biotissues at IR regions, except for wavelengths near 3 and 6 μm , where the initial absorption coefficient is very high.

Acknowledgments

The authors thank the US Office of Naval Research (grant N00014-94-1-1023), and the Russian Foundation of Basic Research (grants 02-02-16855, 00-02-16263) for financial support.

References

1. E. N. Sobol, *Phase Transformations and Ablation in Laser-Treated Solids*, Wiley and Sons, New York (1995).
2. J. Tribble, D. Lamb, L. Reinisch, and G. S. Edwards, "Dynamics of gelatin ablation due to free electron-laser irradiation," *Phys. Rev. E* **55**, 7385–7389 (1997).
3. G. S. Edwards, "Laser desorption and ablation," in *Experimental Methods in the Physical Sciences*, Vol. 30, J. C. Miller, R. F. Haglund, R. Celotta, and T. Lucatorto, Eds., Academic Press, New York (1998).
4. D. Comper, "Physicochemical aspects of cartilage extra-cellular matrix," in *Cartilage: Molecular Aspects*, B. Hall and S. Newman, Eds., CRC Press, Boca Raton, FL (1991).
5. H. Rehanian, A. M. Jamieson, L.-H. Tang, and L. Rosenberg, "Hydrodynamic properties of proteoglycan subunit from bovine nasal cartilage. Self-association behavior and interaction with hyaluronate studied by laser light scattering," *Biopolymers* **18**, 1727–1747 (1979).
6. A. M. Jamieson, J. Blackwell, H. Rehanian, H. Ohno, R. Gupta, et al., "Thermal and solvent stability of proteoglycan aggregates by quasielastic laser light-scattering," *Carbohydr. Res.* **160**, 329–341 (1987).
7. S. Ghosh and W. F. Reed, "New characteristic signatures from time-dependent static light-scattering during polymer depolymerization with application to proteoglycan subunit degradation," *Biopolymers* **35**, 435–450 (1995).
8. A. Sviridov, E. Sobol, V. Bagratashvili, N. Bagratashvili, A. Omelchenko, A. Dmitriev, A. Shechter, Y. Ovchinnikov, V. Svistushkin, G. Nikiforova, N. Jones, and J. Lowe, "Dynamics of optical and mechanical properties of cartilage at laser heating," *Proc. SPIE* **2923**, 114–117 (1996).
9. B. J. F. Wong, T. E. Milner, B. Anvari, A. Sviridov, A. Omelchenko, V. Bagratashvili, E. Sobol, and J. S. Nelson, "Thermo-optical response of cartilage during feedback-controlled laser-assisted reshaping," *Proc. SPIE* **2970**, 380–391 (1997).
10. I. S. Kovach and K. A. Athanasiou, "Small-angle HeNe laser light scatter and the compressive modulus of articular cartilage," *J. Orthop. Res.* **15**, 437–441 (1997).
11. G. S. Edwards, B. J. Johnson, J. Kozub, J. Tribble, and K. Wagner, "Biomedical applications of free-electron lasers," *Opt. Eng.* **32**(02), 314–319 (1993).
12. E. Sobol, M. Kitai, N. Jones, A. Sviridov, T. Milner, and B. Wong, "Heating and structure alterations in cartilage under laser radiation with regard of water evaporation," *IEEE J. Quantum Electron.* **35**, 532–539 (1999).
13. G. Edwards, R. Logan, M. Copeland, L. Reinisch, J. Davidson, B. Johnson, R. Maclunas, M. Mendenhall, R. Ossoff, J. Tribble, J. Werkhaven, and D. O'Day, "Tissue ablation by a free-electron laser tuned to the amide II band," *Nature (London)* **371**, 416–419 (1994).
14. R. Brinkmann, J. Kampmeier, U. Grotehusmann, A. Vogel, N. Koop, M. Asiyo-Vogel, and R. Birngruber, "Corneal collagen denaturation in laserthermokeratoplasty," *Proc. SPIE* **2681**, 56–62 (1996).
15. J. Kampmeier, B. Radt, R. Birngruber, and R. Brinkmann, "Thermal and biomechanical parameters of porcine cornea," *Cornea* **19**, 355–363 (2000).
16. J. Pearce and S. Thomsen, "Rate process analysis of thermal damage," in *Optical-Thermal Response of Laser-Irradiated Tissue*, pp. 551–606, A. J. Welch and M. J. C. van Gemert, Eds., Plenum Press, New York (1995).
17. T. N. Glenn, S. Rastegar, and S. L. Jacques, "Finite element analysis of temperature controlled coagulation in laser irradiated tissue," *IEEE Trans. Biomed. Eng.* **43**, 79–87 (1996).